Thermochimica Acta 507–508 (2010) 21–26

Contents lists available at ScienceDirect

Thermochimica Acta

journal homepage: www.elsevier.com/locate/tca

# Room temperature reaction between uranyl nitrate hexahydrate and rubidium nitrate and polymerisation during denitration of rubidium uranyl nitrate at elevated temperatures

Bhupesh B. Kalekar*, K.V. Rajagopalan, P.V. Ravindran

*Analytical Chemistry Division, Bhabha Atomic Research Centre, Mumbai 400 085, India*

ARTICLE INFO

*Article history:*
Received 3 March 2010
Received in revised form 23 April 2010
Accepted 29 April 2010
Available online 6 May 2010

*Keywords:*
High level nuclear waste
Calciner
Denitration
Nitrato-complex formation
Evolved gas analysis (EGA)

ABSTRACT

The interaction between uranyl nitrate hexahydrate (UNH) and rubidium nitrate in solid state at elevated temperatures has been studied for several compositions using simultaneous thermal analysis techniques (TG–DTA–EGA), X-ray diffraction and IR spectral measurements. The formation of rubidium uranyl nitrate has been observed in rubidium nitrate rich mixtures even at ambient temperature during mixing of the two nitrates in solid state. The reaction at room temperature was incomplete in mixtures containing higher than 30 mol% uranyl nitrate hexahydrate. Thermal and XRD data on equimolar mixture indicate complete dehydration of uranyl nitrate hexahydrate by 300 °C to form rubidium uranyl nitrate, $Rb[UO_2(NO_3)_3]$, which decomposes on further heating to the polymerised structures, $Rb_2[(UO_2NO_3)_2(O)_2]$ and $Rb_4[(UO_2)_3(O)_4(NO_3)_2]$ above 360 °C and 460 °C, respectively. $Rb_4[(UO_2)_3(O)_4(NO_3)_2]$ reacts with $UO_3$ above 550 °C to form rubidium diuranate, $Rb_2U_2O_7$, when the initial nitrate mixture is prepared from compositions containing UNH at 50 mol% or lower levels. In the case of initial nitrate mixtures containing a higher amount of UNH, however, $Rb_2U_4O_{13}$ and $U_3O_8$ are formed above 550 °C.

## 1. Introduction

Nitrates of rubidium and uranium are constituents of the high level liquid waste of spent nuclear fuels along with other fission, corrosion and actinide products [1]. Procedures targeted at isolation of these components to ensure their fixation with a view to confine the activity in the stable forms have been the subject of many discussions in the literature. Donnet et al. [2] studied the adsorption of rubidium on a column using natural mordenite. High temperature reactions of rubidium nitrate with silica, alumina and metakaoline were investigated by Mukerji and Kanyal [3] in the context of waste immobilization programme. Synthesis and decomposition schemes of mixed nitrato complexes of rubidium and rare earths as well as uranium and cesium have been the subject of earlier investigations [4,5].

The study of multiphasic interactions between various nitrates of high level nuclear waste at high temperatures is of interest in the context of determining suitable calcination conditions for conversion of nitrate to oxide form. These studies, taken together with the available information on the decomposition of the individual component nitrates [6–8], are expected to provide useful data for designing calciner for denitration of nuclear waste.

Our earlier studies [9] on elevated-temperature reaction between uranyl nitrate hexahydrate (UNH) and sodium nitrate evidenced the formation of the dimerised nitrato-complex involving oxygen-bridged uranyl ions as an intermediate during the denitration to form sodium diuranate. On the other hand, the mixtures of UNH and strontium nitrate did not interact directly, though $UO_3$, formed by decomposition of UNH, interacted with molten strontium nitrate to give various nitrato complexes which decomposed to strontium uranates [10]. The varied nature of interactions in these pseudobinary systems necessitates detailed studies on other binary, ternary and multicomponent nitrate mixtures to help interpret the reactions occurring during the denitration of high level liquid waste. The reaction between UNH and rubidium nitrate at high temperatures has been studied in this context and the results are presented here.

## 2. Experimental

UNH was prepared from nuclear grade $U_3O_8$ and characterized as described elsewhere [11]. Rubidium nitrate was prepared by crystallization from a solution of rubidium chloride (Fluka AG, Germany) in conc. nitric acid. The salt was recrystallised repeatedly from nitric acid until the filtrate tested negative for chloride test. It was then dried in a desiccator over sodium hydroxide pellets and characterized by X-ray diffraction data and DTA peaks for phase transitions [12,13]. Rubidium uranyl nitrate was also prepared from

---

* Corresponding author. Tel.: +91 22 25593291; fax: +91 22 25505151.
*E-mail address:* bhupkal@barc.gov.in (B.B. Kalekar).

0040-6031/$ – see front matter © 2010 Elsevier B.V. All rights reserved.
doi:10.1016/j.tca.2010.04.024

solution route according to the method reported by Gatehouse and Comyns [14] in order to compare with the product of the solid state reaction between UNH and rubidium nitrate.

Mixtures of UNH with rubidium nitrate containing 20, 30, 40, 50, 60, 70 and 80 mol% UNH were prepared by mixing and grinding gently using a mortar and pestle to ensure a uniform mixture of the two nitrates. The TG–DTA–EGA measurements were carried out on 100 mg samples of the mixtures in argon atmosphere (flow rate: 80 mL/min) using Netzsch thermal analyser (model STA-409) coupled to a quadrupole mass spectrometer (QMG-311, Balzers) via a heated capillary [11]. The specimen holders were made from recrystallised alumina and a heating rate of 10 K/min was maintained in all measurements. The intermediate compounds for XRD measurements were prepared in situ in the thermal analyser by heating the mixtures to the desired temperatures followed by natural cooling of the samples to room temperature under argon flow. All XRD measurements were carried out on a Philips X-ray Diffractometer (model PW1710) using nickel-filtered Cu Kα radiation. Infrared spectra of the residues were recorded in Nujol mull in the wave number range of 200–4000 $cm^{-1}$ on FTIR spectrometer (Model MB102, Bomem, Canada) using cesium iodide windows.

## 3. Results

The DTA data obtained for rubidium nitrate matched well with that reported by Charsley et al. [12]. The XRD data for the prepared sample also corresponded with that reported in literature [13]. The TG, EGA and room-temperature XRD data for the mixture containing 20 mol% UNH are shown in Fig. 1. The XRD pattern corresponded to that for a mixture of rubidium uranyl nitrate and rubidium nitrate. The TG curve does not show the initial dehydration steps of uranyl nitrate hexahydrate. EGA data indicates initiation of denitration only above 360 °C. The weight loss and accompanying NO evolution peak above 640 °C correspond to the decomposition of rubidium nitrate present in excess of equimolar composition.

The results presented in Fig. 2 for thermal behaviour of 50 mol% UNH mixture show that the evolution of nitric oxide from the mixture initiates at 360 °C, nearly 100 °C higher than that in the case of 100 mol% UNH [11] indicating stabilization of the nitrate against thermal decomposition through the formation of a complex nitrate. The TG weight loss data suggest that rubidium uranyl nitrate is formed by 300 °C. This is further confirmed by the concordance of the room-temperature XRD patterns of rubidium uranyl nitrate prepared by solution route and residue of the mixture heated up to 300 °C and then cooled to room temperature (Fig. 3a and b).

The multiple nitric oxide evolution peaks for 50 mol% UNH mixture in the temperature ranges, 360–460 °C, 460–550 °C and 550–620 °C indicate denitration through successive polymerisation reactions of the nitrato complexes (Fig. 2). IR spectral data for samples of the mixture heated up to 460 °C and 550 °C and then cooled to room temperature under argon flow are given in Table 1. Fig. 3c and d shows room-temperature XRD patterns of 50 mol% UNH mixture heated to 460 °C and 550 °C, respectively, which are distinctly different from that of rubidium uranyl nitrate. Thermal, XRD and IR spectral data indicate polymerisation of rubidium uranyl nitrate above 360 °C through oxygen-bridged structures, $Rb_2[(UO_2NO_3)_2(O)_2]$ and $Rb_4[(UO_2)_3(O)_4(NO_3)_2]$ before its final decomposition to rubidium diuranate. The residue of the 50 mol% mixture heated to 620 °C and cooled to room temperature has yielded the XRD pattern (Fig. 3e) corresponding to rubidium diuranate.

The DTA pattern of 80 mol% UNH mixture presented in Fig. 4a shows similarity with that for 100 mol% UNH pattern [11] except for the last endotherm in the temperature range of 580–640 °C corresponding to the decomposition of $UO_3$ to $U_3O_8$. Room-temperature XRD pattern of the residue of 80 mol% UNH mixture (Fig. 4b) heated to 620 °C confirmed the formation of the stable oxides, $Rb_2U_4O_{13}$ and $U_3O_8$.

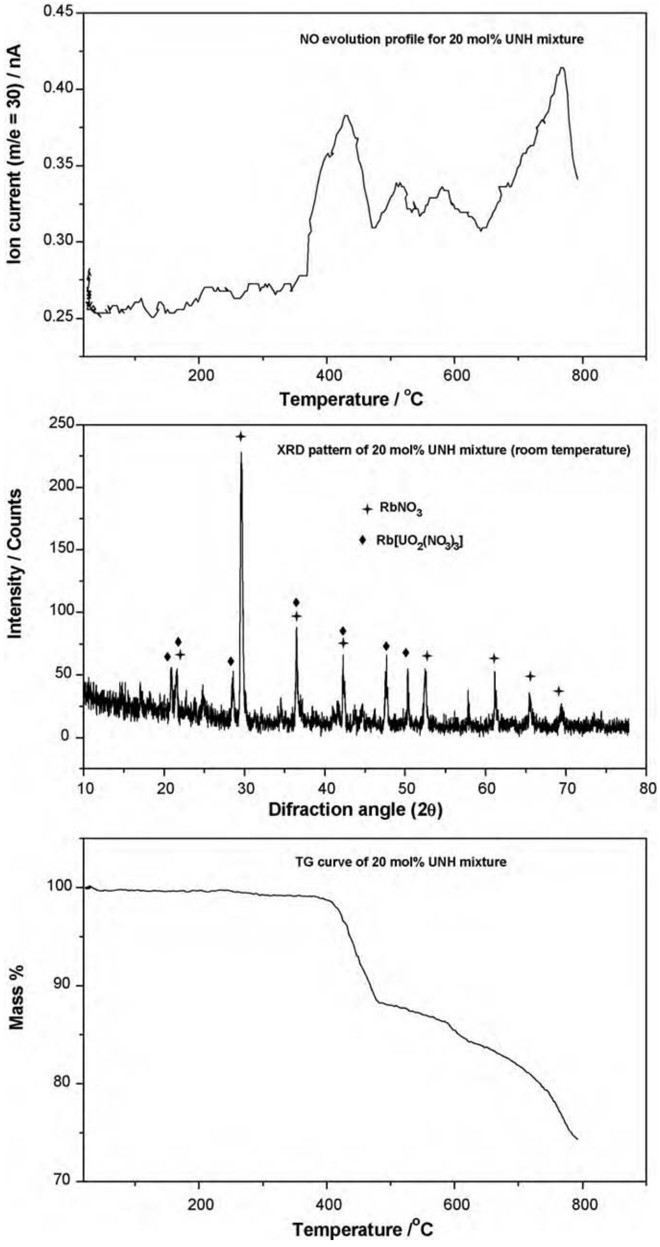

**Fig. 1.** XRD data for 20 mol% UNH mixture prepared at room temperature and TG and EGA data recorded in argon atmosphere on the same sample.

## 4. Discussion

### 4.1. *Interaction of uranyl nitrate hexahydrate with rubidium nitrate*

The TG, XRD and EGA data presented in Fig. 1 clearly show that UNH reacted with rubidium nitrate at room temperature while mixing of the two nitrate powders using a mortar and pestle. Similar results were also observed for mixtures containing 30 mol% UNH. However, for mixtures with higher UNH content, TG and DTA data in the temperature range of 50–250 °C (Fig. 2) indicated occurrence of dehydration steps in UNH [11] and hence the presence of unreacted UNH in the mixture at room temperature.

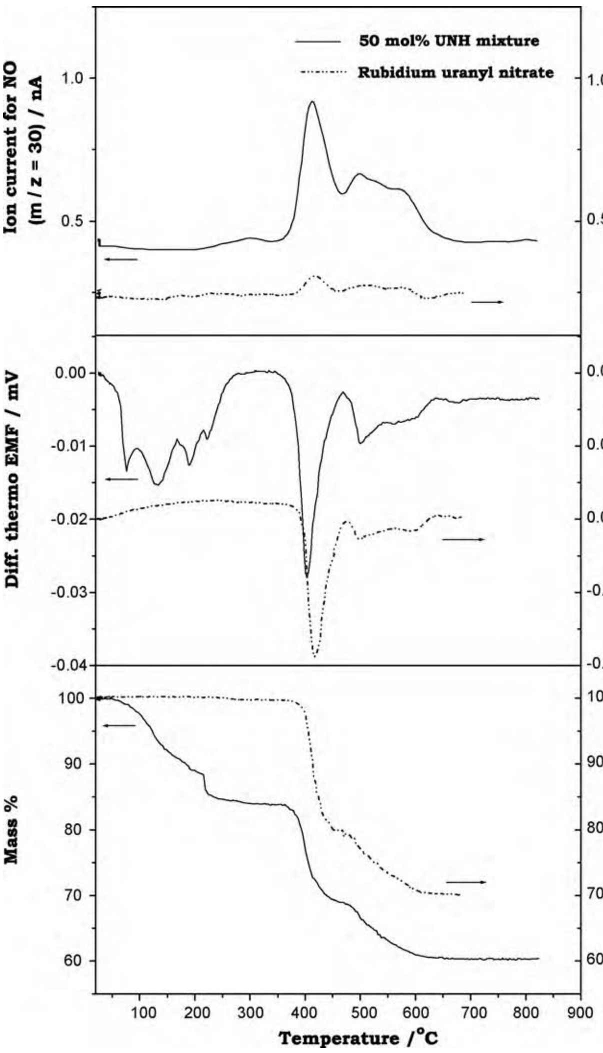

**Fig. 2.** TG–DTA–EGA patterns of 50 mol% UNH mixture and rubidium uranyl nitrate at heating rate of 10 K/min under argon flow.

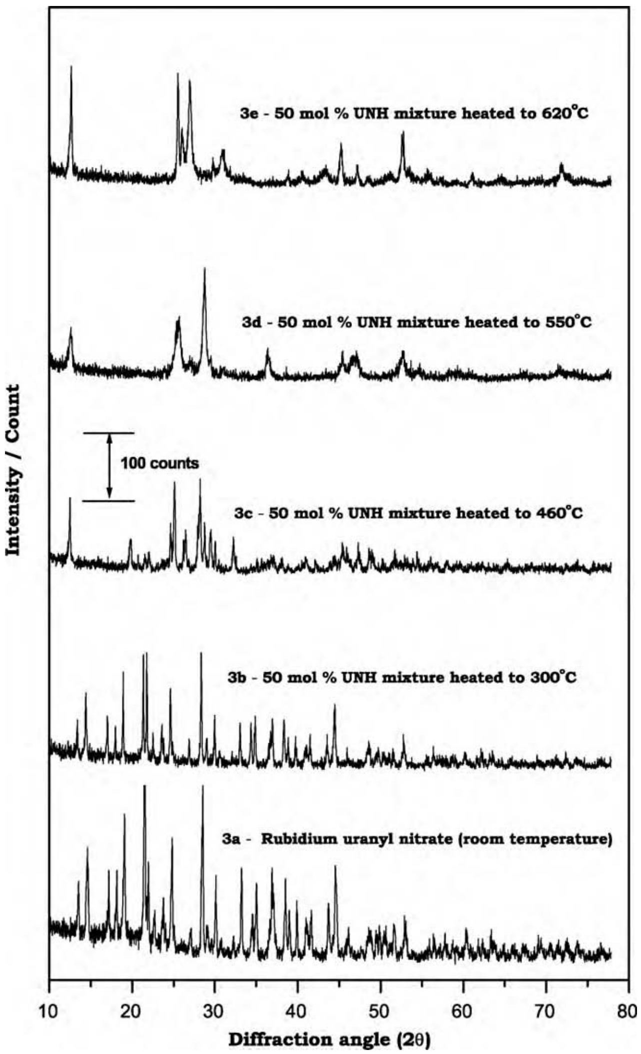

**Fig. 3.** XRD patterns recorded for rubidium uranyl nitrate at room temperature and 50 mol% UNH mixture heated in thermobalance under argon flow to various temperatures and then furnace cooled to room temperature.

In the case of 50 mol% UNH mixture, the dehydration events in UNH are evidenced by the endothermic weight loss steps in the temperature range 50–250 °C. A closer examination of EGA data presented in Fig. 2 also reveals a small NO evolution hump in the temperature range 250–325 °C which corresponds to the temperature range for the first denitration step during decomposition of UNH. The very small weight loss step on the TG curve in this temperature range, indicated by drifting weight level, is indicative of the presence of a small amount of unreacted uranyl nitrate hexahydrate. Similar results were also observed with progressively more prominent endothermic weight loss step accompanied by NO evolution in this temperature range for compositions rich in uranyl nitrate hexahydrate. These results show that the reaction between uranyl nitrate hexahydrate and rubidium nitrate at room temperature is incomplete when the component nitrates are present in compositions that are richer than 30 mol% in uranyl nitrate hexahydrate. The latter composition corresponds to a mixture with almost equal weight percent of the two component nitrates. Hence, under the condition of identical particle size, facilitated by mixing and grinding the powder samples uniformly, the number of reactant particles of the two components is likely to be identical in 30 mol% UNH mixture. The number of $RbNO_3$ particles surrounding UNH particles will be higher for compositions containing less than 30 mol% UNH. In view of the better contact of UNH particles with $RbNO_3$ under these conditions, the reaction of UNH with rubidium nitrate at room temperature will be more efficient and complete than in UNH rich mixtures. The endothermic dehydration of unreacted UNH at and above 25 °C in UNH rich mixtures will also provide a moist and self-cooled environment that might decrease the rate of reaction between the two nitrates.

Since the reaction between UNH and rubidium nitrate to form rubidium uranyl nitrate is equimolar in nature, the case 50 mol% mixture provided a clearer insight into the reaction mechanism on heating the mixture. TG curve of the 50 mol% mixture showed a total endothermic weight loss of 15.6% in the temperature range of 50–250 °C. Simultaneously recorded EGA curve showed prominent evolution of nitric oxide only above 360 °C. Hence, the weight loss observed in the temperature range 50–250 °C should be attributed to loss of water molecules from UNH. The observed weight loss corresponded to the removal of all six molecules of water from UNH constituent in the equimolar mixture and indicated absence of hydroxynitrate formation, unlike in the case of 100 mol% UNH samples [11]. The delayed nitric oxide evolution and absence of hydroxynitrate formation in the case of the mixture evidenced formation of a nitrate complex, which was thermally more stable than UNH. On the basis of TG–DTA–EGA results, the following reaction

**Table 1**
IR data recorded for the residues of equimolar mixture heated to 460 °C and 550 °C.

| $cm^{-1}$ | Peak assignment | References |
|---|---|---|
| 460 °C | | |
| 227 | M–O vibration | [17] |
| 247, 279 | $UO_2^+$ deformation | [18] |
| 459, 474 | M–O–N vibration | [17] |
| 553 | M–O–M vibration | [18] |
| 721 | $\nu_5$-$NO_2$ asym. bend | [17] |
| 770 | $\nu_5$-$NO_2$ sym. bend | [19] |
| 850 | $\nu_2$-(out of plane) $NO_3^-$ ion | [19] |
| 891 | $UO_2^+$ asym. strech | [18] |
| 972, 1035 | $\nu_2$-N–O stretch | [19] |
| 1153, 1168 | $\nu_4$-$NO_3$ ion | [19] |
| 1377 | $\nu_3$-$NO_2$ asym. strech | [19] |
| 226 | M–O vibration | [17] |
| 550 °C | | |
| 247, 279, 302 | $UO_2^+$ deformation | [18] |
| 326, 341, 398, 420 | M–O–N vibration | [17] |
| 567 | M–O–M vibration | [17] |
| 721 | $\nu_5$-$NO_2$ asym. bend | [17] |
| 831, 841 | $\nu_2$-($NO_3$ ion out of plane) | [17] |
| 896, 943 | $UO_2^+$ asymmetry stretch | [18] |
| 973, 1035 | $\nu_2$-N–O stretch | [19] |
| 1153, 1168 | $\nu_4$-$NO_3$ stretch | [19] |
| 1299 | $\nu_1$-$NO_3$ stretch covalent | [17] |
| 1379 | $\nu_3$-$NO_2$ asym. strech | [19] |
| 1460 | $\nu_4$-$NO_3$ ion | [17] |
| 1506, 1521 | $\nu_4$-$NO_2$ asym. stretch | [17,19] |
| 1541 | $\nu_2$-N–O stretch | [17] |

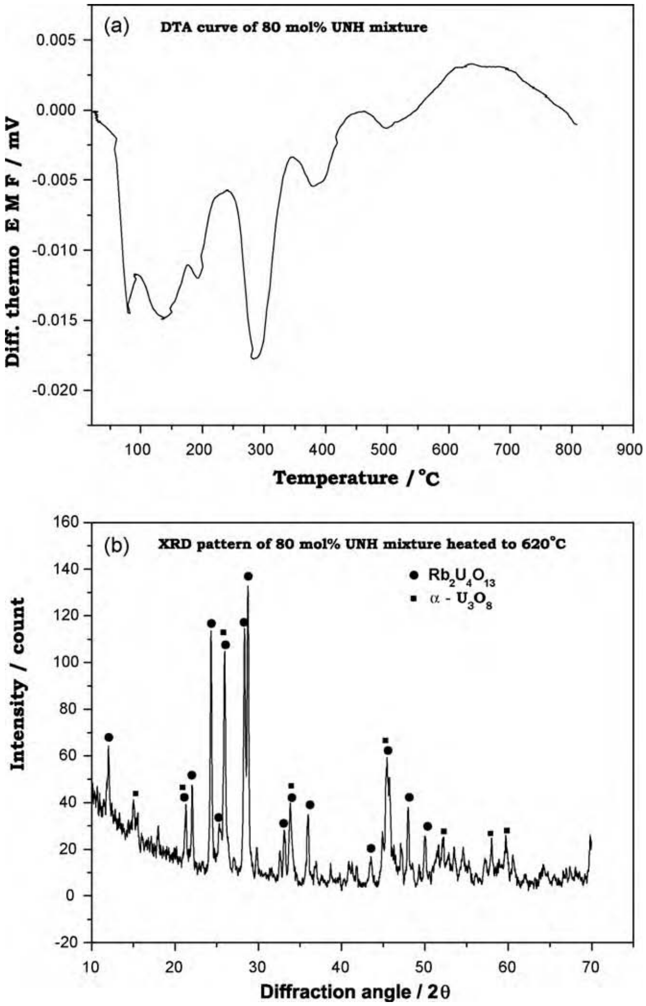

**Fig. 4.** DTA of 80 mol% UNH mixture heated in argon atmosphere and room temperature XRD pattern of the same mixture heated to 620 °C and then furnace cooled to room temperature.

is proposed.

$$UO_2(NO_3)_2 \cdot 6H_2O + RbNO_3 \xrightarrow{50–250\,°C} Rb[UO_2(NO_3)_3] + 6H_2O \qquad (1)$$

The nature of the nitrate complex was also evaluated by comparing room-temperature XRD patterns for a sample of freshly crystallized rubidium uranyl nitrate and the residue obtained by heating the mixture up to 300 °C followed by cooling the same under argon flow to room temperature. The diffraction peaks obtained for freshly crystallised rubidium uranyl nitrate in Fig. 3a matched well with those recorded for a residue of the mixture heated to 300 °C and cooled to room temperature (Fig. 3b) and also with the literature data [15] for $Rb[UO_2(NO_3)_3]$. The results of TG–DTA–EGA and XRD measurements confirmed the formation of the rubidium uranyl nitrate by 300 °C from the mixture. This complex was thermally stable up to 360 °C as indicated by the constant weight plateau region on TG curve of the mixture. Rubidium uranyl nitrate samples prepared by the solution route and from the mixture showed same thermal behaviour above 360 °C leading to identical intermediate nitrato complexes and stable mixed oxide (Fig. 2). A shift of denitration endotherms for rubidium uranyl nitrate to slightly high temperature in comparison with the mixture is possibly because of the effect of experimental variables (e.g., quantity of rubidium uranyl nitrate which is higher for freshly crystallized sample in view of absence of water of crystallization) on DTA curve and heterogeneity of 50 mol% UNH mixture.

### 4.2. *Polymerisation of rubidium uranyl nitrate*

DTA curve of the 50 mol% UNH mixture showed an endotherm in the temperature range of 360–460 °C with a peak temperature of 405 °C. Simultaneously recorded EGA curve of the mixture showed evolution of nitric oxide in the same temperature range and hence this thermal event is attributed to a denitration step. The peak area covered under the NO evolution peak for equimolar mixture was much larger than that for any other composition of UNH and rubidium nitrate. This revealed that the complex formation was favoured in the equimolar mixtures. The room-temperature XRD data for the residue of the mixture heated to 460 °C presented in Fig. 3c showed a major peak at the 2$\theta$ value of 25.13° which was absent in the case of rubidium uranyl nitrate. Further, the appearance of some new peaks corresponding to the 2$\theta$ values at 19.81°, 26.22°, 26.44° and 32.21° indicated the formation of a new crystalline phase. The pattern in Fig. 3c could be indexed to a monoclinic system with the cell parameters of $a$ = 4.594 Å, $b$ = 14.164 Å, $c$ = 18.684 Å and $\beta$ = 117.01°. These results do not match with any of the reported XRD data for nitrates in rubidium nitrate–uranyl nitrate system [15,16]. The infrared spectral data obtained on this residue (Table 1) showed M–O–N vibrations in the range below 500 $cm^{-1}$. The IR absorption in the range 570–550 $cm^{-1}$ can be assigned to U–O–U stretching vibrations of the oxygen-bridged species [17]. The IR data also indicated the presence of the nitrates [17–19]. Simultaneous TG–DTA–EGA measurements also confirmed the occurrence of two additional denitration events in the temperature ranges of 460–550 °C and 550–620 °C. The multiple nitric oxide evolution peaks in the temperature ranges, 360–460, 460–550 and 550–620 °C indicate the formation of polymerised nitrato complexes through successive denitration reactions.

The TG curve for the equimolar mixture exhibited a weight loss of 14.9% in the temperature range of 360–460 °C. The TG–DTA–EGA, XRD and IR spectral data indicated the formation of dimerised rubidium uranyl oxynitrate, $Rb_2[(UO_2NO_3)_2(O)_2]$, in this temperature range according to the following reaction:

$$2Rb[UO_2(NO_3)_3] \xrightarrow{360–460\,°C} Rb_2[(UO_2NO_3)_2(O)_2] + 2NO + 2NO_2 + 2O_2 \qquad (2)$$

Theoretical and actual weight losses are in reasonable agreement considering the overlap of the TG weight loss steps in the temperature ranges of 360–460 °C and 460–550 °C. The structure of dimerised rubidium uranyl oxynitrate can be presented as,

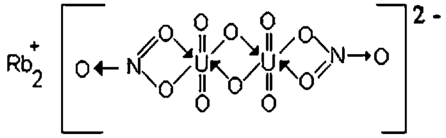

Similar structures have earlier been proposed to interpret the thermoanalytical data for the reaction between sodium nitrate and UNH [9].

The TG curve for the 50 mol% UNH mixture indicated a weight loss of 6.0% in the temperature range of 460–550 °C. The room-temperature XRD pattern (Fig. 3d) obtained for the residue of the mixture heated to 550 °C and cooled to room temperature under argon flow showed new peaks at the $2\theta$ values of 25.59°, 36.36° and 52.70°. The XRD pattern showed most intense peak at 28.75° and did not match those for rubidium uranates or any known nitrate in the rubidium–uranium–nitrate system. The pattern in Fig. 3d could be indexed to a monoclinic system with the cell parameters of $a = 3.663$ Å, $b = 16.605$ Å, $c = 7.832$ Å and $\beta = 98.76°$. The IR spectral data recorded for this heated residue of the mixture indicated an increase in the metal oxygen vibrations below 500 cm$^{-1}$ (Table 1) compared to the residue of mixture at 460 °C and showed bands due to nitrates. This could be indicative of the presence of additional units of oxygen-bridged uranyl ions due to enhanced level of polymerisation. On the basis of TG–DTA–EGA, XRD and IR spectral data, the following reaction is proposed, viz.,

$$2Rb_2[(UO_2NO_3)_2(O)_2] \xrightarrow{460\text{–}560\,^{\circ}C} Rb_4[(UO_2)_3(O)_4(NO_3)_2] + UO_3 + NO + NO_2 + O_2 \quad (3)$$

The presence of $UO_3$ could not be confirmed from the XRD pattern recorded for the mixture at 550 °C probably because it was present in amorphous form [20] and masked by peaks of crystalline nitrato complex. The experimental weight loss obtained for this reaction is slightly higher than theoretical weight loss. This is because of the inaccuracy in reading the weight loss, contributed by overlap of TG steps in the temperature ranges of 360–460 °C and 460–550 °C. It is interesting to note that the total experimental weight loss of 20.9% in the temperature range of 360–550 °C matched well with theoretical weight loss for formation of $Rb_4[(UO_2)_3(O)_4(NO_3)_2]$ from $Rb[UO_2(NO_3)_3]$. The enhanced level of polymerisation in rubidium nitrate–UNH mixture as compared to sodium nitrate–UNH mixture [9] may be due to the higher electropositive nature of rubidium than sodium. The present set of data also suggests an increase in the extent of polymerisation with temperature. The structural formula of trimerised rubidium uranyl oxynitrate may be presented as,

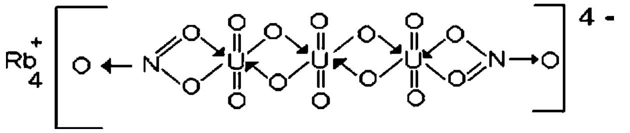

TG curve of the equimolar mixture indicated weight loss of 3.0% in the temperature range of 550–620 °C accompanied by NO evolution as evidenced by EGA data presented in Fig. 2. Apparently, the polymerised complex, $Rb_4[(UO_2)_3(O)_4(NO_3)_2]$ and $UO_3$ of mixture reacted above 550 °C to give rubidium diuranate.

$$Rb_4[(UO_2)_3(O)_4(NO_3)_2] + UO_3 \xrightarrow{550\text{–}620\,^{\circ}C} 2Rb_2U_2O_7 + NO + NO_2 + O_2 \quad (4)$$

The observed weight loss was in agreement with the theoretical value for the proposed reaction. The XRD pattern obtained for the residue of the mixture heated to 620 °C in Fig. 3e showed the presence of rubidium diuranate phase [21].

The reactions in UNH deficient compositions are similar up to 550 °C as evident from Fig. 1. The reaction indicated by Eq. (4) above, however, overlaps with the decomposition of unreacted rubidium nitrate and the denitration event extends up to 800 °C with an additional NO evolution peak at 765 °C for 20 mol% UNH mixture.

In the case of UNH rich compositions, the endothermic peaks in the temperature range of 230–580 °C closely resembled the DTA peaks reported for UNH in the corresponding temperature range (Fig. 4a). This is because the amount of rubidium uranyl nitrate formed is relatively small. In the case of 80 mol% UNH mixture, presented in Fig. 4, only 20 mol% of UNH had undergone reaction with $RbNO_3$ due to which the thermal events in rubidium uranyl nitrate formed are small in intensity. These low intensity signals merge into the tails of peaks for denitration reactions in UNH (60 mol%) remaining unreacted with $RbNO_3$. The final endotherm corresponding to the conversion of $UO_3$ to $U_3O_8$ in the temperature range of 580–640 °C observed in the case of UNH was, however, not clearly observed for the mixture possibly because of removal of $UO_3$ through reaction with $Rb_4[(UO_2)_3(O)_4(NO_3)_2]$. The room-temperature XRD carried out on the residue obtained at 620 °C (Fig. 4b), however, evidenced the formation of $Rb_2U_4O_{13}$ [22] and $\alpha$-$U_3O_8$ [23] rather than $Rb_2U_2O_7$ observed in the case of equimolar mixture. Apparently, $Rb_4[(UO_2)_3(O)_4(NO_3)_2]$ formed according to equation (3) reacted with excess $UO_3$ to form $Rb_2U_4O_{13}$ and $\alpha$-$U_3O_8$ in accordance with the equation,

$$Rb_4[(UO_2)_3(O)_4(NO_3)_2] + 13UO_3 \xrightarrow{550\text{–}620\,^{\circ}C} 2Rb_2U_4O_{13} + \tfrac{8}{3}U_3O_8 + NO + NO_2 + \tfrac{7}{3}O_2 \quad (5)$$

## 5. Conclusions

Thermal and XRD measurements on mixtures containing 70 mol% or more $RbNO_3$ indicate the formation of rubidium uranyl nitrate by reaction between the two nitrates even at ambient temperature. The interaction between UNH and rubidium nitrate at elevated temperatures shows that the nitrato-complex formation is favoured in mixture of 1:1 mol ratio. The intermediate, rubidium uranyl nitrate is polymerised through oxygen-bridged structures, like, $Rb_2[(UO_2NO_3)_2(O)_2]$ and $Rb_4[(UO_2)_3(O)_4(NO_3)_2]$, above 360 °C and 460 °C, respectively. The resulting nitrato-complex, $Rb_4[(UO_2)_3(O)_4(NO_3)_2]$ and $UO_3$ react above 550 °C to give a stable oxide, rubidium diuranate. The mixtures rich in UNH content also reacted to form $Rb_4[(UO_2)_3(O)_4(NO_3)_2]$ which reacted with $UO_3$ (present in larger proportion) to form $Rb_2U_4O_{13}$.

## Acknowledgement

The authors thankfully acknowledge the help from Dr. A.K. Tyagi, Head, Structural Chemistry Section, Chemistry Division, BARC in the use of XRD facility.

## References

[1] International Atomic Energy Agency, Techniques for the solidification of HLW, Technical Report Series 176, IAEA, Vienna, 1979, p. 10.
[2] L. Donnet, Y. Morita, I. Yamagishiand, M. Kubota, Japan Atomic Energy Research Institute, JAERI-Research 98-058, 1998.
[3] J. Mukerji, P.B. Kanyal, Bhabha Atomic Research Centre, Report – BARC – 691, 1973.
[4] N. Guillon, J.P. Auffrédic, D. Louër, J. Solid State Chem. 122 (1996) 59–67.
[5] S.R. Bhardwaj, M.S. Chandrashekharaiah, Thermochim. Acta 71 (1983) 247–255.
[6] W.W. Wendlandt, Anal. Chim. Acta 15 (1956) 435–439.
[7] K.S. Chunn, Atomic Energy Establishment, Report – AERE – R 8735, 1977.
[8] C.A. Strydom, C.P. Jan Vurent, J. Therm. Anal. 32 (1987) 157–160.
[9] B.B. Kalekar, K.V. Rajagopalan, C.G.S. Pillai, P.V. Ravindran, P.K. Mathur, J. Nucl. Mater. 279 (2000) 245–252.
[10] P.V. Ravindran, B.B. Kalekar, K.V. Rajagopalan, C.G.S. Pillai, P.K. Mathur, J. Nucl. Mater. 317 (2003) 109–116.
[11] K.V. Rajagopalan, P.V. Ravindran, T.P. Radhakrishnan, J. Therm. Anal. 44 (1995) 89–96.
[12] E.L. Charsley, J.P. Davis, E. GlÖggler, N. Hawkins, T. Lever, K. Peters, M.J. Richardson, I. Rothemund, A. Stegmayer, J. Therm. Anal. 40 (1993) 1405–1444.

[13] JCPDS International Centre for Diffraction Data, Powder Diffraction file 1995, Card no. 17-516.
[14] B.M. Gatehouse, A.E. Comyns, J. Chem. Soc. (1958) 3965–3971.
[15] JCPDS International Centre for Diffraction Data, Powder Diffraction file 1995, Card no.79-0709.
[16] JCPDS International Centre for Diffraction Data, Powder Diffraction file 1995, Card no.74-2069.
[17] J.R. Ferraro, Low Frequency Vibrations of Inorganic Compounds, Plenum, New York, 1971, pp. 78–80.
[18] A. Anderson, C. Chieh, D.E. Irish, J.P.K. Tong, Can. J. Chem. 58 (1980) 1651–1658.
[19] B.M. Gatehouse, S.E. Livingstone, R.S. Nyhlom, J. Chem. Soc. (1971) 4222.
[20] R.S. Ondrejcin, T.P. Garrett Jr., J. Phys. Chem. 65 (1961) 470–473.
[21] JCPDS International Centre for Diffraction Data, Powder Diffraction file 1995, Card no. 29-1106.
[22] JCPDS International Centre for Diffraction Data, Powder Diffraction file 1995, Card no. 29-1107.
[23] JCPDS International Centre for Diffraction Data, Powder Diffraction file 1995, Card no. 47-1493.